JTTEE5 13:586-592
DOI: 10.1361/10599630421505
1059-9630/$19.00 © ASM International

Peer Reviewed

Effect of Particle Morphology on Flow Characteristics of a Composite Plasma Spray Powder

Malcolm K. Stanford, Christopher DellaCorte, and Daniel Eylon

(Submitted December 24, 2002; in revised form July 2, 2003)

The effects of BaF_2-CaF_2 particle morphology on National Aeronautics and Space Administration (NASA) PS304 feedstock powder flowability were investigated. BaF_2-CaF_2 eutectic powders were fabricated by comminution (producing an angular morphology) and by gas atomization (producing a spherical morphology). The fluoride powders were added incrementally to the other powder constituents of the NASA PS304 feedstock, (Ni-Cr, Cr_2O_3, and Ag powders). A linear relationship between flow time and concentration of the BaF_2-CaF_2 powder was found. The flow of the powder blend with spherical BaF_2-CaF_2 was better than that with angular BaF_2-CaF_2. The flowability of the powder blend with angular fluorides decreased linearly with increasing fluoride concentration. However, the flow of the powder blend with spherical fluorides was independent of fluoride concentration. The results suggest that for this material blend, particle morphology plays a significant role in flow behavior, offering potential methods to improve powder flowability and enhance the commercial potential. These findings may be applicable to other difficult-to-flow powders such as cohesive ceramics.

Keywords: coatings, particle morphology, plasma spray coatings, powder flowability, solid lubrication

1. Introduction

The eutectic composition of barium fluoride and calcium fluoride (BaF_2-30wt.%CaF_2) is a solid lubricant that is used in National Aeronautics and Space Administration (NASA) PS304 feedstock (hereafter referred to as PS304), a plasma spray deposited, composite, solid-lubricant coating for friction and wear reduction in turbomachinery applications (Ref 1-6). PS304 is made from a powder blend consisting of Ni-Cr, Cr_2O_3, and Ag, and eutectic BaF_2-CaF_2 powders. Experience with the blended powder feedstock for this coating has indicated that the particle size of the fluoride constituent has a significant effect on the flowability of the PS304 powder blend. This investigation studied eutectic BaF_2-CaF_2 powders with different morphologies produced by two powder fabrication techniques, comminution and gas atomization. The objective of this study was to establish the role of eutectic particle morphology in PS304 powder blend flowability to improve feedstock properties and to enhance its commercial potential. The fabrication techniques in this study are limited to the production of primary particles and exclude spray-dried agglomerates. Previous research has shown that spray-dried particles can have flow problems associated with particle surface roughness (Ref 7). Particle porosity and the addition of a binder in agglomerates also may have an adverse effect on the performance of the coating system. The data generated in this study are unique to PS304, but the results are expected to have a broader application in other classes of composite powder blends.

Malcolm K. Stanford and **Daniel Eylon,** University of Dayton, Dayton, OH 45469–0121; and **Christopher DellaCorte,** National Aeronautics and Space Administration, Glenn Research Center, Cleveland, OH 44135. Contact e-mail: Malcolm.K.Stanford@nasa.gov.

2. Background

The PS304 plasma spray coating was developed at the NASA Glenn Research Center (Ref 8) for the reduction of sliding friction and wear in turbomachinery applications at temperatures from subambient up to 650 °C. The composition of this coating is 60 wt.% nichrome (Ni-20wt.%Cr), 20 wt.% chromia (Cr_2O_3), 10 wt.% Ag, and 10 wt.% eutectic BaF_2-CaF_2. Nichrome serves as a binder and provides wear resistance, and Cr_2O_3 is for wear resistance. Silver and BaF_2-CaF_2 are solid lubricants at low temperatures and high temperatures, respectively.

The plasma spray process propels particles through a plasma flame that is produced by the ionization of inert or molecular gases (Ref 9). The plasma heats the particles above their melting temperature. Molten particles then impact the substrate, where they quickly solidify. The buildup of subsequent particles adds thickness to the developing coating. The feedstock is typically a powder that is used to facilitate control of the rapid melting and resolidification of the coating material. Where multicomponent coating systems are to be deposited, the feedstock can be a powder blend of the coating constituents.

In a preliminary study, it was found that feedstock powder for PS304 would intermittently clog in the plasma spray feed hopper due to the presence of BaF_2-CaF_2 particles under 50 μm in size (Ref 10).

Calcium fluoride and barium fluoride may be mined or synthesized by wet chemistry. The largest deposits of calcium fluoride are in China, Mexico, and South Africa (Ref 11). The bulk of these deposits are used for steel flux, the production of alu-

minum, and the production of hydrofluoric acid. High-purity fluorides are used for optics and for high-temperature lubricants. They are typically produced by wet chemistry due to the cost involved in removing impurities from mined materials. The material is precipitated from a calcium- or barium-rich solution with fluorine gas. This process yields very fine fluoride particles (~1 μm) that are extremely difficult to transfer using standard bins and hoppers due to their high surface area, which promotes agglomeration. To improve powder handling, the precipitated product may be fused and subsequently produced in a size that is more easily processed. To fabricate BaF_2-CaF_2 powders, the two constituents must be fused, and the bulk material must be converted to a powder.

Conventional fabrication of ceramic powder can be achieved with a number of comminution processes. Unfortunately, these processes yield particles that are irregular and angular in shape, with poor flow characteristics compared with smoother, more rounded particles (Ref 12). Both the size and the shape of the powder particles are believed to affect the flowability of the powder blends. This study examines the effect of the fluoride shape on the flow characteristics of PS304 feedstock powder.

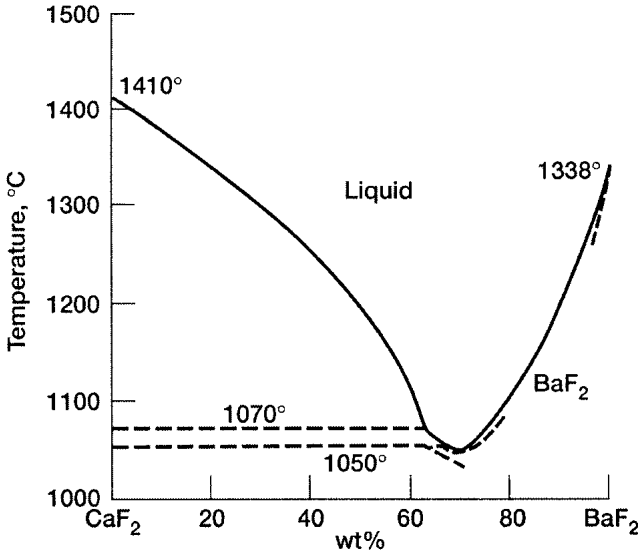

Fig. 1 Binary phase diagram for BaF_2-CaF_2. Source: Ref 22

3. Powder Flow and Powder Fabrication

As particles in a powder system get smaller, they have a greater tendency to agglomerate rather than to fall away under the influence of gravity (Ref 13). This is due to the fact that the surface area of the particles becomes large in proportion to their mass. Therefore, the surface forces of friction and cohesion begin to dominate gravitational forces as particle size decreases, reducing the flowability of the powder.

Particle shape also affects the flow characteristics of powders (Ref 12). As a particle departs from a low-energy geometry such as a sphere, the ratio of its surface area to its volume increases. Depending on the fabrication method, particles can take on many different shapes, including spherical, rounded, and angular.

The flowability of a powder can be quantified by measuring its gravity-driven flow rate through a calibrated orifice. The conventional method measures the time (in seconds) required for a 50 g sample to flow through a standardized funnel (Ref 14). Grey and Beddow (Ref 15) studied the flow characteristics of copper powders with spherical, irregular, and flake morphologies, and showed that, as the shape became less spherical, the flow properties were degraded. Little work has been published on the flow characteristics of spherical ceramic powders because ceramics, owing to their generally high melting temperatures, are typically angular due to the fact that they are fabricated by traditional comminution processes.

The level of interparticle friction in a powder can be estimated from the apparent density, which is the bulk density as poured and without agitation (Ref 12). As interparticle friction increases, apparent density decreases.

Comminution (crushing) processes reduce the size of a material by the application of a combination of compressive and shear forces (Ref 16). These processes take advantage of the naturally occurring defects in ceramic materials such as grain boundaries, pores, and microcracks, as well as their inherent brittleness (Ref 17).

The dependence of the fracture strength of a brittle particle on a preexisting flaw is described by the well-known Griffith relationship (Ref 18). It states that the fracture strength σ_f of a material is inversely proportional to the square root of the flaw size c:

$$\sigma_f = \sqrt{\frac{2\gamma_f \cdot E}{\pi c}}$$

where E is the modulus of elasticity of the material and γ_f is the energy required to create two new fracture surfaces. When the stress on a particle due to comminution is greater than σ_f, fracture and size reduction will take place. Due to their brittle nature, the powders will be angular.

Comminution can be a very inefficient and energy-intensive process despite the brittle nature of ceramics (Ref 19). This is especially true for the production of fine powders in which, with each particle fragmentation, flaw population and size decrease. When there are fewer and smaller flaws, comminution energy is expended in particle deformation and heat generation.

All commercial applications of PS304 to date have used fluorides produced by comminution. For this study, a development project was implemented to also produce spherical fluorides. The high energy required to melt ceramics typically makes fusion-based processes undesirable. However, the melting temperatures of fluorides are relatively low despite their highly ionic bonding character (Ref 20, 21). As shown in Fig. 1, CaF_2 melts at 1410 °C, and BaF_2 melts at 1338 °C (Ref 22). Furthermore, at a composition of 70 wt.% BaF_2 and 30 wt.% CaF_2, a eutectic is formed that melts at just below 1050 °C. This composition was selected for the current application due to the ease of processing afforded by the reduced melting point, which also enabled the use of gas atomization for the fabrication of novel spherical BaF_2-CaF_2 particles.

The principle elements of a gas-atomization process are shown schematically in Fig. 2 (Ref 23, 24). Molten material is

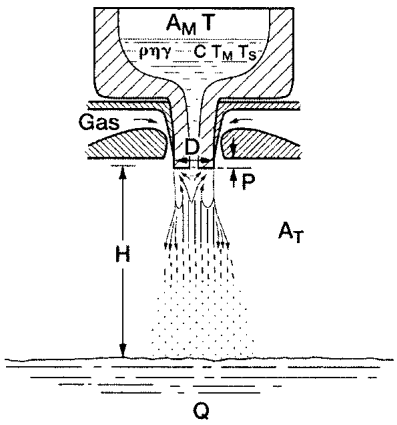

Atmosphere	During melting (A_M)
	In atomizing tank (A_T)
	Temperature (T)
Molten Material	Chemistry (C)
	Viscosity (η)
	Surface tension (γ)
	Melting temperature (T_M)
	Superheat (T_S)
	Density
	Nozzle diameter (D)
Atomizing Fluid	Pressure (P)
	Flow rate
	Velocity
Tank Parameters	Flight path (H)
	Quenching medium (Q)

Fig. 2 Main elements of an atomization process. Source: Ref 23, 24

contained in a tundish, which has a nozzle with an inner diameter *D*. The difference between the processing temperature and the melting point of the material is the superheat, which prevents the material from freezing prematurely. The molten material is allowed to flow through the nozzle under the influence of gravity. As the liquid stream exits the nozzle, the pressure drop created by the flow of the atomizing fluid and the impact of the gas stream causes the stream to disintegrate. The surface tension of the molten material encourages the formation of rounded or spherical droplets (Ref 25). The droplets then cool and solidify, forming particles as they fall to a collection tank at a distance *H* below the nozzle.

4. Experimental Procedure

Nichrome particles (Fig. 3a) are 44 to 74 μm in size (Table 1) and have a rounded shape resulting from water atomization (Ref 23, 24). Cr_2O_3 particles (Fig. 3b) are 30 to 44 μm in size (Table 1) and have an angular morphology. This powder was fabricated by sintering the bulk material into large bricks and then comminuting the bricks into a powder. The spherical silver, particles (Fig. 3c), fabricated by gas atomization, are 45 to 100 μm in diameter. The sizes and shapes of the Ni-Cr, Cr_2O_3, and Ag powder particles were available as commercial products and were not modified in this study.

To produce the BaF_2-CaF_2 eutectic, shown in Fig. 3(d), 70 wt.% BaF_2 and 30 wt.% CaF_2 were combined in a graphite crucible and were melted under vacuum at 1100 °C followed by vacuum cooling. The solidified material then was removed from the crucible for powder fabrication by the two methods.

In the first stage of the size reduction of the particles in the angular powder, large chunks of the fused fluoride material were fed into a jaw crusher that compresses the material between two opposing and inclined surfaces. One surface is fixed and the other reciprocates, providing the crushing force. Once the material is small enough to fit through the gap at the bottom of the two crushing surfaces, it is collected in a bin. This size-reduction step produces a coarse powder that is similar to fine gravel.

To further reduce the angular fluoride powder size, the powder retrieved from the jaw crusher was then fed into a disk mill. A disk mill feeds the powder between two opposing disk surfaces. One disk is stationary, while the other rotates. The disks have teeth that run along their radii to fracture the particles trapped between them. The teeth allow less space for the particles as they reach the outer edge of the disks such that the minimum gap determines the largest particle that will fall between the disks.

The atomization of the fluorides was performed with a commercially available small-scale, close-coupled gas-atomization system (Ref 26). Approximately 1400 g of 150 μm fluoride eutectic powder was obtained for atomization. The feedstock was induction-melted under an argon cover in a high-purity graphite crucible at 200 °C superheat. The crucible also acted as the susceptor for the induction power. The melt was bottom-tapped from the crucible directly into the atomization nozzle. Argon of commercial purity was used for the atomization gas, and a secondary quench of deionized water was used to cool and confine the nascent powder. Powder was retrieved from the quenching medium by settling and decanting. The concentrated powder then was washed in acetone, decanted, and dried at a low temperature (below 100 °C). About 99% of the crucible charge was recovered as powder.

The fluoride powders were classified by screening according to ASTM standard specification B 214-99. The screening instrument uses a vertically oscillating column of air and a combination of vertical and horizontal tappers to separate the particles according to size (Table 1).

The flow rate of each powder blend was measured twice according to ASTM standard B 213-97. For this measurement, a 50 g sample of the powder blend being tested was loaded into a Hall flowmeter. A schematic of the apparatus is shown in Fig. 4. The Hall flowmeter was found to be a reliable indicator of the flowability of the powder blends through the powder feed system of the studied plasma spray system. The Hall flowmeter has been used in recent studies to characterize the flow rate of plasma spray feedstock powders (Ref 7, 27).

For each flow test, a powder blend consisting of 60 g of Ni-Cr, 20 g of Cr_2O_3, 10 g of silver, and an incrementally increasing amount of fluoride powder with either angular or spherical particles was prepared by mixing the constituents together in a 125 mL high-density polyethylene bottle until the powder was well blended. A 50 g sample was obtained from this powder blend for flow testing. The time it took the entire 50 g sample to exit the

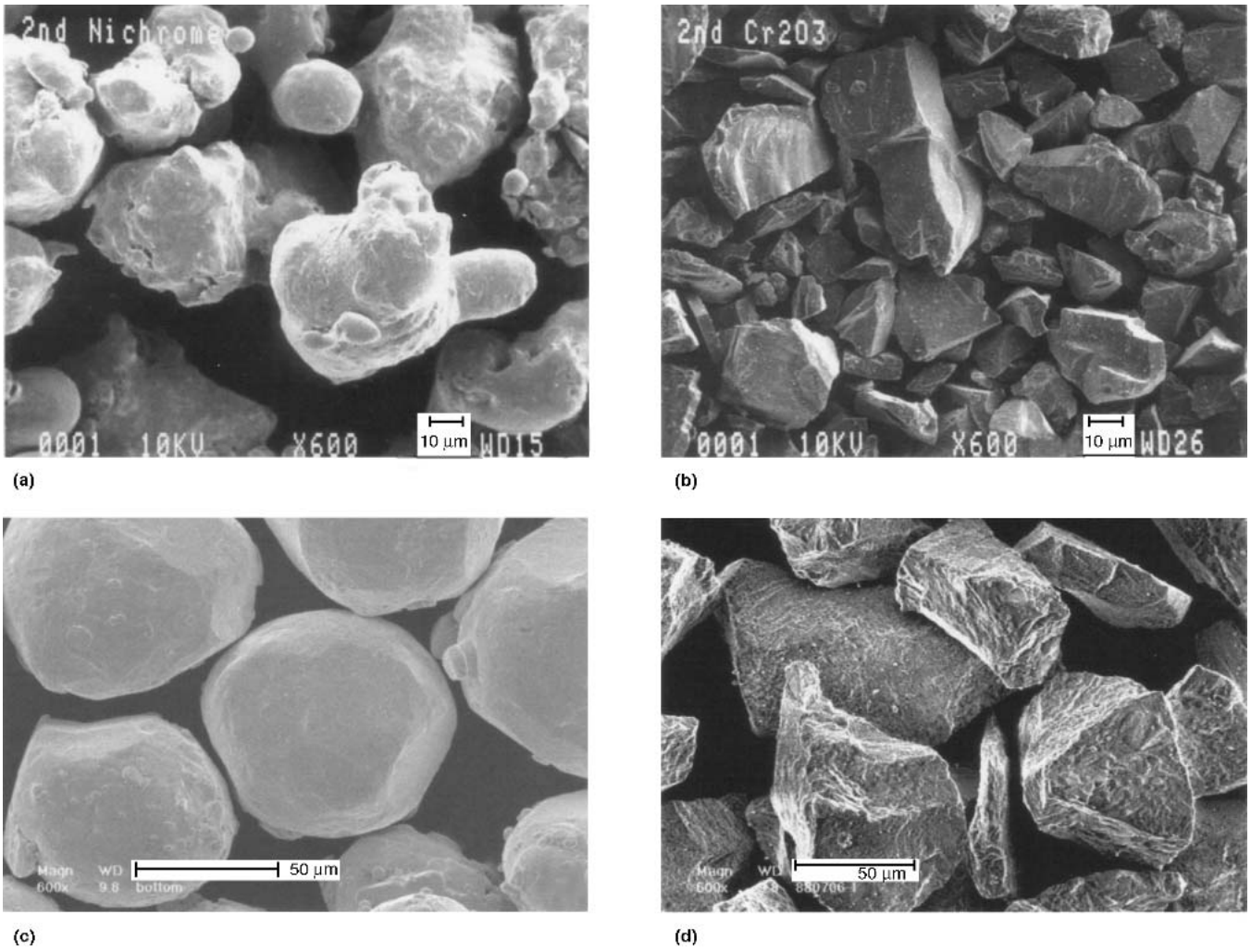

Fig. 3 Representative shapes of the particles in the powders in PS304 used in this study (original magnification 600×). (a) Rounded Ni-Cr. (b) Angular Cr_2O_3. (c) Spherical silver. (d) Angular fluoride

Table 1 Summary of feedstock properties

Properties	Fluoride ($70BaF_2$-$30CaF_2$) Angular	Fluoride ($70BaF_2$-$30CaF_2$) Spherical	Ni-Cr (80Ni-20Cr)	(Cr_2O_3)	Ag
Fabrication method	Comminution	Gas atomization	Water atomization	Comminution	Gas atomization
Surface morphology	Angular	Spherical	Rounded	Angular	Spherical
Particle size distribution	45-106 µm	45-106 µm	44-74 µm	30-44 µm	45-100 µm
Theoretical density, g/cm^3	4.01	4.01	8.57	5.22	10.49

funnel, the flow time, was then measured. The amount of fluoride powder used in the blend then was increased by 1.0 g, and the test was repeated. This procedure was repeated from 0 up to 10 wt.% fluoride. Data were reported on a plot of flow time versus the weight percent of fluoride in the powder blend. Tests were performed at room temperature and 50% relative humidity.

5. Results and Discussion

Figure 5 shows scanning electron micrographs of the fluoride powders with angular and spherical particles. The particles collected from the jaw crusher were smaller than 2 mm. The particles collected from the disk mill were smaller than 200 µm. The crushed and ground fluoride particles had an angular shape. The surfaces of these particles had fracture patterns that were consistent with brittle fracture.

The particles produced by atomization had a spherical shape. The surfaces of the particles showed equiaxed grains, which is characteristic of a material that has undergone rapid solidification (Ref 12). The surfaces of the particles were generally smooth, with a few attached satellites from smaller particles that collided with the larger ones before they were completely solidi-

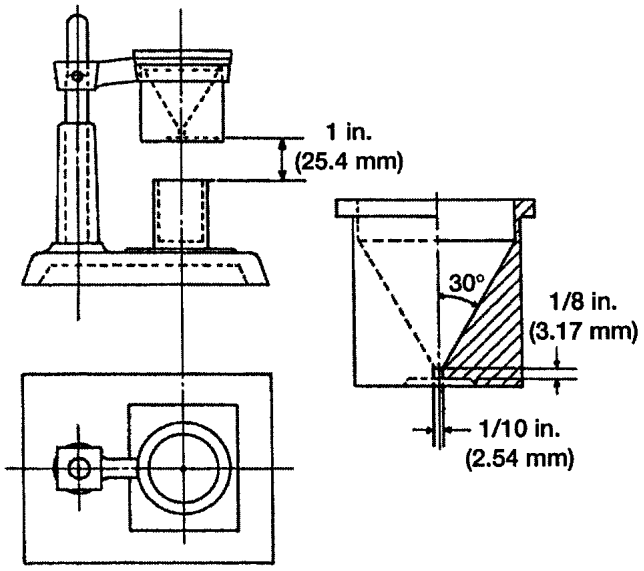

Fig. 4 Flowmeter setup. Source: Ref 23

fied. The particle diameters had a log-normal distribution that ranged from 0.82 to 124 μm, as determined by the light-blockage particle-size-analysis technique (Ref 28). The median particle diameter was approximately 17 μm. This particle size distribution was composed of more fines than expected based on the experience of the powder manufacturer with similar materials.

The weight percentages of the comminuted and atomized fluoride powders collected per screening run are shown in Fig. 6(a) and (b), respectively. The remaining powder was collected on the pan beneath the No. 325 sieve. Due to their aspect ratio, some particles were able to fit through the screens by their smallest dimension. Since screening was used to classify the powders, the surface-to-volume ratio of the angular fluoride particles was nearly the same as that of the spherical fluoride particles. Therefore, the observed effect of particle morphology on flowability will be separate from the effect of the ratio of surface area to volume.

An equal particle size distribution by mass of −140 +325 mesh (45-106 μm) powders was prepared of comminuted and atomized fluoride particles (Table 1). The fluoride powders were added incrementally to a powder blend consisting of 60 g of Ni-Cr, 20 g of Cr_2O_3, and 10 g of silver. The reported flow time is the average value from two consecutive tests. The results are shown graphically in Fig. 7.

The flow times of the powder with the spherical fluoride particles was always lower than the powder with the angular fluoride particles. The relationship between the flow time of the powder blend with respect to increasing fluoride content was linear over the range from 0 to 10 wt.%. The variability in the flow time measurement at each weight percent of fluoride, based on two runs per test condition, was typically less than 0.5%. Variability with angular fluoride particles was slightly higher than that with spherical fluoride particles. Error bars are not shown on the plot (Fig. 7) because they do not span the width of the data labels. The flow times of the powder blend using the angular powder particles fit a line described by $y = 0.5094x +$ 26.303, where y and x represent flow time and fluoride concentration, respectively. The correlation coefficient was $R^2 =$ 0.9896. The flow times of the powder blend with the spherical powder particles fit a line described by $y = -0.003636x + 26.41$. The correlation coefficient was $R^2 = 0.0068$, indicating that there was essentially no relationship between spherical fluoride concentration and flow time. The intercept of the line approximates the flow time at 0 wt.% fluoride. By statistical hypothesis testing, the intercepts of both lines could not be distinguished from the measured value (26.3 s). In addition, the slope of the line representing the blend with spherical fluorides was impossible to differentiate from zero.

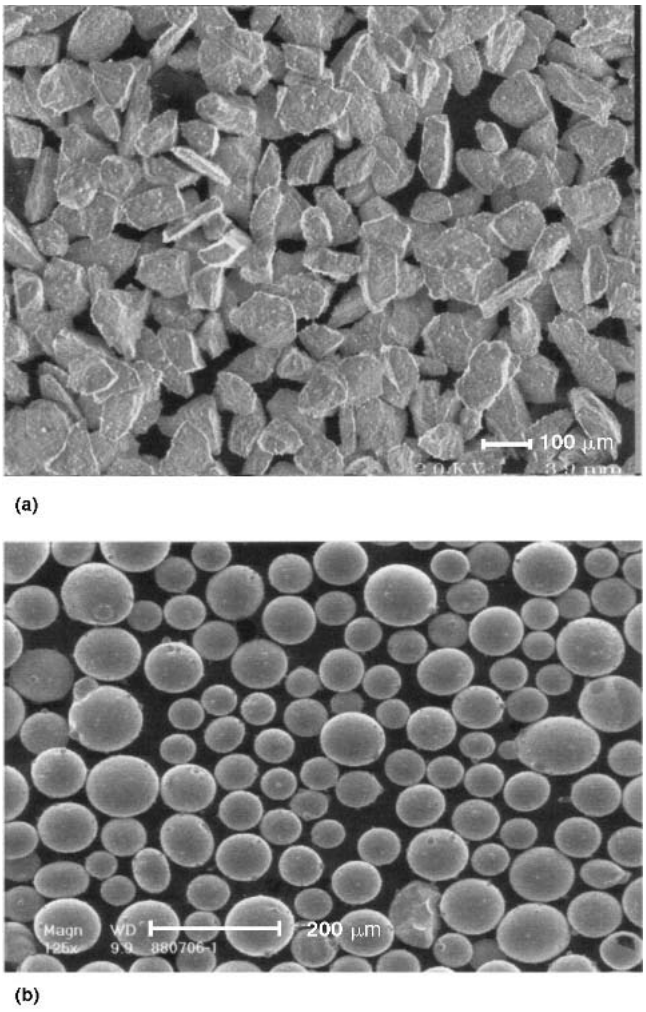

Fig. 5 Angular and spherical fluoride powders used in this study (original magnification 125×). (a) Angular particles of fluoride powder fabricated by comminution. (b) Spherical particles of fluoride powder fabricated by atomization

Based on the rule of mixtures (in which density is given by

$$\rho_{blend} = \sum_i v_i \rho_i$$

where the volume fraction v_i is a function of the weight fraction of constituent i, assuming no interaction between particles), the

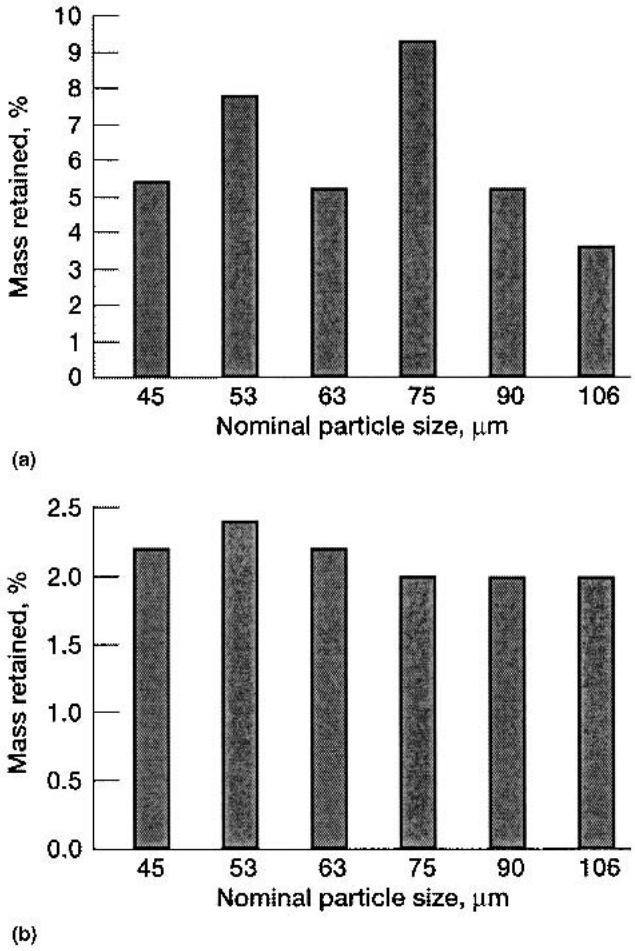

Fig. 6 Mass yield of BaF_2-CaF_2 powders from sieving procedure. (a) Comminuted fluoride particles. (b) Atomized fluoride particles

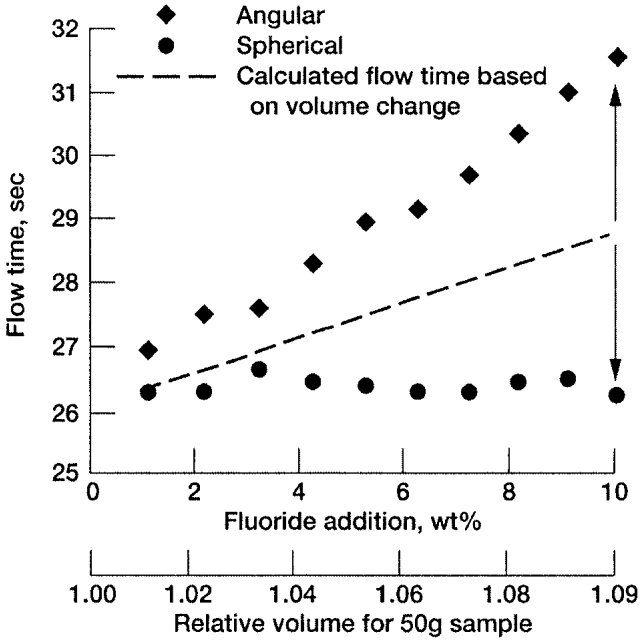

Fig. 7 Plot of funnel flow time versus fluoride weight percent

volume of a standard 50 g powder sample of PS304 feedstock powder is expected to increase with increasing fluoride content because the theoretical density of the fluoride, 4.01 g/cm^3, is less than those of the other constituents. The densities of Ni-Cr, Cr_2O_3, and Ag are 8.57, 5.22, and 10.49 g/cm^3, respectively (Table 1). If the flow time of the powder blend was only dependent upon the volume of powder transferred though the funnel with no particle interaction effects, the flow time of a 50 g sample with 10 wt.% fluoride would be expected to take 9% longer than a 50 g sample with no fluorides, due to the 9% increase in volume for the 50 g sample (see the secondary *x*-axis in Fig. 7). The calculated flow times based only on increased volume are represented by the dashed line in Fig. 7. The powder blend with 10 wt.% angular fluoride particles would then have a flow time of about 29 s, as shown by the calculated line, instead of the measured 31.6 s if volume alone was considered. Based on this, the measured flow time using angular fluoride particles was approximately 9% higher than expected. This difference is thought to be due to the increased interparticle friction and its resulting increase on the void fraction in the powder blend. Using spherical fluoride particles, the flow time was independent of the fluoride concentration. In this case, the effects of interparticle friction and reduction of powder density were offset by the improvement in flow given by the spherical fluorides.

To confirm the increase in volume with fluoride concentration, the apparent density of the powders was measured at 0 and 10 wt.% fluoride. The apparent density of the PS304 powder with 10 wt.% of either fluoride type was nearly 5% lower than that for the powder blend containing only Ni-Cr, Cr_2O_3, and Ag. This measurement is the reciprocal specific volume and accounts for the interparticle friction that is present in the powder blend both before and after the fluoride constituent was added. Clearly, the increase in the flow time after the addition of the fluoride particles is proportional to the decrease in apparent density of the powder blend. However, the decreased density alone does not fully account for the increased flow time.

A probable explanation for the difference in flow characteristics is the particle morphology. Irregularly shaped particles have relatively poor flow characteristics due to higher surface area, which results in higher interparticle friction (Ref 12). The flat surfaces of the angular fluoride particles tend to provide much greater effective contact area with adjacent particles. On the other hand, spherical fluoride particles are most likely to have point contact with other particles; therefore, angular fluoride particles are expected to have higher interparticle friction. In addition, the irregular shape makes interaction with adjacent particles more random than the more regularly shaped spherical particles, which might explain the slightly higher variability observed in the measurements of the flow times of the powder blends containing angular fluorides. Furthermore, the spherical fluoride particles are better able to roll against the other powder constituents. Since rolling friction is typically lower than sliding friction, the powder blends with angular fluoride particles would tend to have higher interparticle friction. In every case studied, the fluoride powders with spherical particles offered flow properties that were significantly better than the fluoride powders

with angular particles, which appears to be closely linked to the effect of particle morphology on interparticle friction.

6. Summary and Conclusions

The objective of this investigation was to identify the effects of BaF_2-CaF_2 powder particle morphology on the flow characteristics of PS304 feedstock. Based on the results of this study, these conclusions can be made:

- Fluoride particle morphology has a significant effect on powder flow. Improved PS304 powder blend flow properties can be obtained using fluoride powder with spherical particles in place of the fluoride powder with angular particles that is currently used.
- Increased flow time for powder blends containing *angular* fluoride particles was linearly proportional to the weight percentages of fluoride in the 0 to 10 wt.% range.
- Argon gas atomization of eutectic BaF_2-CaF_2 can be successfully used to fabricate powder with spherical particles. Based on these findings, there may be other relatively low-melting-point engineering ceramics that could be fabricated by gas atomization. This would be of great benefit to processes that presently rely on ceramic powders with angular particles that tend to be subjected to the effects of interparticle cohesion and friction.
- The flow times of the PS304 feedstock with spherical fluoride particles are essentially independent of fluoride concentration. This finding is underscored by the fact that the increase in flow time with increased fluoride concentration that is predicted by the rule of mixtures is not observed for spherical fluoride particles. This behavior is related to the morphology of the fluoride particles.
- The results presented in this study relate specifically to the PS304 solid lubricant powder blend. However, the generalized findings regarding powder fabrication and the effect of morphology on interparticle friction may offer insight into the behavior of other powder blend systems.

References

1. C. DellaCorte, V. Lukaszewicz, M.J. Valco, K.C. Radil, and H. Heshmat, Performance and Durability of High Temperature Foil Air Bearings for Oil-Free Turbomachinery, *Tribol. Trans.,* Vol 43 (No. 4), 2000, p 744-780
2. C. DellaCorte and J.C. Wood, "High Temperature Solid Lubricant Materials for Heavy Duty and Advanced Heat Engines," NASA TM-106570, National Aeronautics and Space Administration Glenn Research Center, 1994
3. J.A. Laskowski and C. DellaCorte, Friction and Wear Characteristics of Candidate Foil Bearing Materials From 25 °C to 800 °C, *Lubr. Eng.,* Vol 52, 1996, p 605-612
4. C. DellaCorte and B.J. Edmonds, "Preliminary Evaluation of PS300: A New Self-Lubricating High Temperature Composite Coating for Use to 800 °C," NASA TM-107056, National Aeronautics and Space Administration Glenn Research Center, 1996.
5. C. DellaCorte, "The Evaluation of a Modified Chrome Oxide Based High Temperature Solid Lubricant Coating for Foil Gas Bearings," NASA/TM-1998-208660, National Aeronautics and Space Administration Glenn Research Center, 1998, available at: http://gltrs.grc.nasa.gov/, accessed Dec 20, 2002
6. C. DellaCorte, "Evaluation of Advanced Solid Lubricant Coatings for Foil Air Bearings Operating at 25 and 500 °C," NASA/TM-1998-206619, National Aeronautics and Space Administration Glenn Research Center, 1998, available at: http://gltrs.grc.nasa.gov/, accessed Dec 20, 2002
7. B.K. Kim, D.W. Lee, and G.H. Ha, Plasma Spray Coating of Spray-Dried Cr_2O_3/3 wt% TiO2 Powder, *J. Thermal Spray Technol.,* Vol 10 (No. 1), 2001, p 133-137
8. C. DellaCorte and B.J. Edmonds, Self-Lubricating Composite Containing Chromium Oxide, U.S. Patent 5,866,518, Feb 2, 1999
9. H.S. Ingham and A.P. Shepard, *Flame Spray Handbook,* Metco, 1965
10. M.K. Stanford, Control of Interparticle Cohesion in PS304 Plasma Spray Deposited Solid Lubricant Coating Powder Feedstock, Ph.D. dissertation, University of Dayton, 2002
11. G.B. McClurg, Fluorspar, *Am. Ceram. Soc. Bull.,* Vol 76 (No. 6), 1997, p 99-101
12. R.M. German, *Powder Metallurgy Science,* Metal Powder Industries Federation, 1984
13. A.D. Zimon, *Adhesion of Dust and Powder,* 2nd ed., Consultants Bureau, 1982
14. "Standard Test Method for Flow Rate of Metal Powders," B 213–97, *Annual Book of ASTM Standards,* Vol 02.05, ASTM, p 26-28
15. R.O. Grey and J.K. Beddow, On the Hausner Ratio and Its Relationship to Some Properties of Metal Powders, *Powder Technol.,* Vol 2, 1969, p 323-326
16. T. Tanaka and Y. Kanda, Crushing and Grinding, *Powder Technology Handbook,* 2nd ed., Marcel Dekker, 1997, p 527-553
17. J.S. Reed, *Introduction to the Principles of Ceramic Processing,* John Wiley & Sons, 1988
18. A.A. Griffith, The Phenomena of Rupture and Flow in Solids, *Philos. Trans. R. Soc. (London), Ser. A,* Vol 221, 1921, p 163-168
19. S.G. Malghan, Comminution, *Ceramics and Glasses,* Vol 4, *Engineered Materials Handbook,* ASM International, 1991, p 75-82
20. D.W. Richerson, *Modern Ceramic Engineering: Properties, Processing, and Use in Design,* Marcel Dekker, 1992
21. L. Pauling, *The Nature of the Chemical Bond and the Structure of Molecules and Crystals: An Introduction to Modern Structural Chemistry,* 3rd ed., Cornell University Press, 1960
22. M. Rolin and M. Clausier, Revue Internationale des Hautes Températures et des Réfractaires, *Bull. Soc. Nat. Fr. Hautes Temp. Réfract.,* Vol 4 (No. 1), 1967, p 42
23. J.K. Beddow, *The Production of Metal Powders by Atomization,* Heyden, London, 1978
24. J.J. Dunkley, Atomization, *Powder Metal Technologies and Applications;* Vol 7, *ASM Handbook,* ASM International, 1998, p 35-52
25. E. Klar and W.M. Shafer, High-Pressure Gas Atomization of Metals, *Powder Metallurgy for High Performance Applications,* John J. Burke and Volker Weiss, Ed., Syracuse University Press, 1972, p 57-68
26. J.T. Strauss, HJE Company, Glens Falls, NY, Personal Communication
27. S.M. Tasirin, The Effect of Fines on Flow Properties of Binary Mixtures, *Chem. Eng. Commun.,* Vol 179, 2000, p 101-115
28. R. Davies, Size Measurement, *Powder Technology Handbook,* 2nd ed., Marcel Dekker, 1997, p 15-42